crystals

MDPI

Article

Lewis Acid Properties of Tetrel Tetrafluorides—The Coincidence of the σ-Hole Concept with the QTAIM Approach

Sławomir J. Grabowski [1,2]

[1] Faculty of Chemistry, University of the Basque Country and Donostia International Physics Center (DIPC), P.K. 1072, 20080 Donostia, Spain; s.grabowski@ikerbasque.org

[2] IKERBASQUE, Basque Foundation for Science, 48011 Bilbao, Spain

Academic Editors: Peter Politzer and Jane S. Murray

Received: 19 January 2017; Accepted: 3 February 2017; Published: 8 February 2017

Abstract: Tetrel bond is analysed for a series of ZF_4 (Z = C, Si, Ge) complexes with one and two NH_3 or AsH_3 ligands. The MP2/aug-cc-pVTZ calculations were performed and supported by results of the Quantum Theory of "Atoms in Molecules" (QTAIM) and the Natural Bond Orbitals (NBO) approaches. The Z-tetrel atoms of complexes analysed interact through their σ-holes with nitrogen or arsenic Lewis base centres; these interactions correspond to the Z–N/As bond paths according to the QTAIM approach. The QTAIM and NBO results show that these interactions are relatively strong and they possess numerous characteristics of covalent bonds. The theoretical analysis is supported by the discussion on crystal structures which are characterized by the same type interactions.

Keywords: tetrel bond; σ-hole; Quantum Theory of "Atoms in Molecules"; Natural Bond Orbital (NBO) method; electron charge density shift

1. Introduction

Various Lewis acid–Lewis base interactions play a key role in different chemical reactions and biological processes [1–3]. The most often investigated hydrogen bond is crucial in numerous such processes [4–7] but there are also other significant interactions; for example, tetrel bond, which may be defined as an interaction between the Group 14 element acting as the Lewis acid centre and a region that is rich of the electron density by a lone electron pair, π-electron system, etc. [8–12]. This interaction is classified as the σ-hole bond [8–10] that is a link between a σ-hole situated in an elongation of one of covalent bonds to the atom considered and the Lewis base centre [13–16]. The σ-hole is a region depleted of the electron density due to its outflow to the internal part of the system, partly to the σ-bond of the centre considered. Hence, this region is often characterized by a positive electrostatic potential (EP). It has been shown that the atoms of Groups 14–17 often possess σ-holes forming with Lewis base centres the σ-hole bonds [13–16]. Recently, the Group 18 elements were also considered as those that may form the σ-hole bonds since they possess regions characterized by positive EPs [17].

There are numerous early studies on the tetrel bond; for example, the theoretical analysis of the SiF_4–NH_3 and SiF_4–$(NH_3)_2$ complexes [18], or the study on various complexes of silicon species with electron-rich groups [19]. The tetrel bond was analysed in terms of the σ-hole concept for the first time by Murray and co-workers in complexes where the σ-hole on silicon or germanium atom is linked with nitrogen centre of the NH_3 or HCN species [8]; in complexes of SiF_4 with amines, larger clusters containing up to three NH_3 molecules were considered [9]. The interplay between the halogen and tetrel bond was discussed [10]; the tetrel bond was considered as a preliminary stage of the S_N2 reaction [12], a computational study of structural and energetic properties of acetonitrile–Group 14 tetrahalide complexes was performed [20]. There is an interesting study on the nature of bonding in

dimers of Lappert's stannylene where the Sn-Sn intermolecular links are observed and where the tin centres play the roles of Lewis acid and Lewis base simultaneously [21].

This study concerns the tetrel bond interaction; five and six coordinated tetrel centres are analysed and it is discussed if all their links possess characteristics of covalent bonds. Very recently, the coordination of tin and lead centres was discussed and it was found that these centres may be classified as pentavalent or even hexavalent ones [22]. This is why it is interesting to analyse if such a situation of covalent in nature interactions occurs for lighter Group 14 elements: carbon, silicon and germanium. One can refer to earlier studies where the coordination of light tetrel centres was analysed; pentacoordinate carbon compounds were analysed experimentally and theoretically by Akiba and co-workers [23,24]; it was discussed if the hexavalent carbon can exist [25]. Pentacoordinate silicon complexes were analysed and the corresponding S_N2 reaction pathways were discussed [26], the crystal structures of penta- and hexacoordinated germanium centres were reported [27,28]; hexacoordinated Ge and Sn centres in crystal structures were also analysed [29].

The ZF_4–NH_3 and ZF_4–$(NH_3)_2$ (Z = C, Si, Ge) complexes are a subject of this study since one can expect strong interactions between Z-tetrels and the NH_3 species that may lead to penta- and hexacoordinated tetrel centres. The same or similar complexes to those chosen here for an analysis were investigated before. One may refer to the above-mentioned early theoretical study on the SiF_4–NH_3 and SiF_4–$(NH_3)_2$ complexes (ab initio MO calculations were performed with the use of STO-3G and STO-6G basis sets) [18]. However, there are other early experimental studies, for example, a diammoniate of silicon tetrafluoride, SiF_4–$(NH_3)_2$, has been prepared in a highly purified form and its X-ray powder diffraction pattern has been measured [30]. The infrared matrix isolation study on the SiF_4–NH_3 adduct was performed, its spectra suggest a trigonal-bipyramidal arrangement about the Si-centre with the NH_3 species in an axial position [31]. One can mention other related studies as the free-jet IR spectroscopy of SiF_4–N_2 and SiF_4–CO complexes [32] or the infrared matrix isolation study on the GeF_4 complexes with oxygen containing bases [33]. The crystal structures of germanium tetrafluoride and tin tetrafluoride complexes with soft thioether coordination were analysed [34]; the complexes of germanium tetrafluoride with phosphane ligands were investigated spectroscopically and in crystal structures [35]. In the latter study, the germanium arsanes were also analysed and the $GeCl_4$ arrangement was found in the crystal structure where the germanium centre is additionally involved in the interaction with two arsenic atoms; thus, it may be considered as the hexacoordinated centre. This is why the GeF_4–AsH_3 and GeF_4–$(AsH_3)_2$ complexes are also analysed here, since in these species the interactions of germanium with halogen and arsenic centres mimic the interactions existing in the above-mentioned crystal structure.

2. Computational Details

The calculations were carried out with the Gaussian09 set of codes [36] using the second-order Møller–Plesset perturbation theory (MP2) [37], and the Dunning style aug-cc-pVTZ basis set [38]. Frequency calculations have confirmed that the obtained structures correspond to energetic minima. To take into account relativistic effects for arsenic and germanium centres, the Stuttgard/Cologne group ECP10MDF pseudopotentials were applied [39] with the corresponding Peterson AVTZ (11s12p10d2f)/[6s5p4d2f] basis sets [40].

The interaction and binding energies, E_{int}s and E_{bin}s, were calculated; E_{int} is the difference between the energy of the complex and the sum of energies of monomers which correspond to their geometries in the complex. In the case of the binding energy, E_{bin}, the energies of isolated monomers not involved in any interactions are taken into account [41]. The deformation energy, E_{def}, defined as the $E_{bin} - E_{int}$ difference [42], is discussed for the complexes analysed. E_{def} is a positive value since the complex formation leads to a change of geometry of monomers that are pushed out from their energetic minima. The basis set superposition error (BSSE) correction [43] was calculated and the BSSE corrected interaction and binding energies are presented and discussed hereafter.

The Quantum Theory of "Atoms in Molecules" (QTAIM) [44,45] was applied to analyse critical points (BCPs) in terms of the electron density (ρ_{BCP}), its Laplacian ($\nabla^2\rho_{BCP}$), the total electron energy density at BCP (H_{BCP}) and the components of the latter value, the kinetic electron energy density (G_{BCP}) and the potential electron energy density (V_{BCP}). The QTAIM calculations were performed with the use of the AIMAll program [46]. The Natural Bond Orbital (NBO) method [47] was also applied to analyse electron charge shifts being the result of complexation as well as orbital–orbital interactions. For the Natural Bond Orbital (NBO) calculations, the NBO 5.0 program [48] implemented in GAMESS set of codes [49] was used.

3. Results and Discussion

3.1. Interaction and Binding Energies

Figure 1 shows molecular graphs of complexes analysed here, where the pentacoordinated tetrel centre is observed, i.e., the complexes of ZF_4 with one ligand, NH_3 or AsH_3. Figure 2 presents, as an example, the molecular graph of the GeF_4–$(AsH_3)_2$ complex that contains two ligands. The simple ZF_4 species as components of complexes were chosen here to analyse the Lewis acid properties of Z-centres that according to previous studies [10] should increase in the following order, C < Si < Ge. It was shown that the fluorine electron withdrawing substituents enlarge the positive electrostatic potential at Group 14 elements [10], similar to that observed for other centres characterized by σ-holes [13–15]. Thus, the tetrel centre in ZF_4 should interact strongly with Lewis bases since the NH_3 species is characterized by strong Lewis base properties of the nitrogen centre.

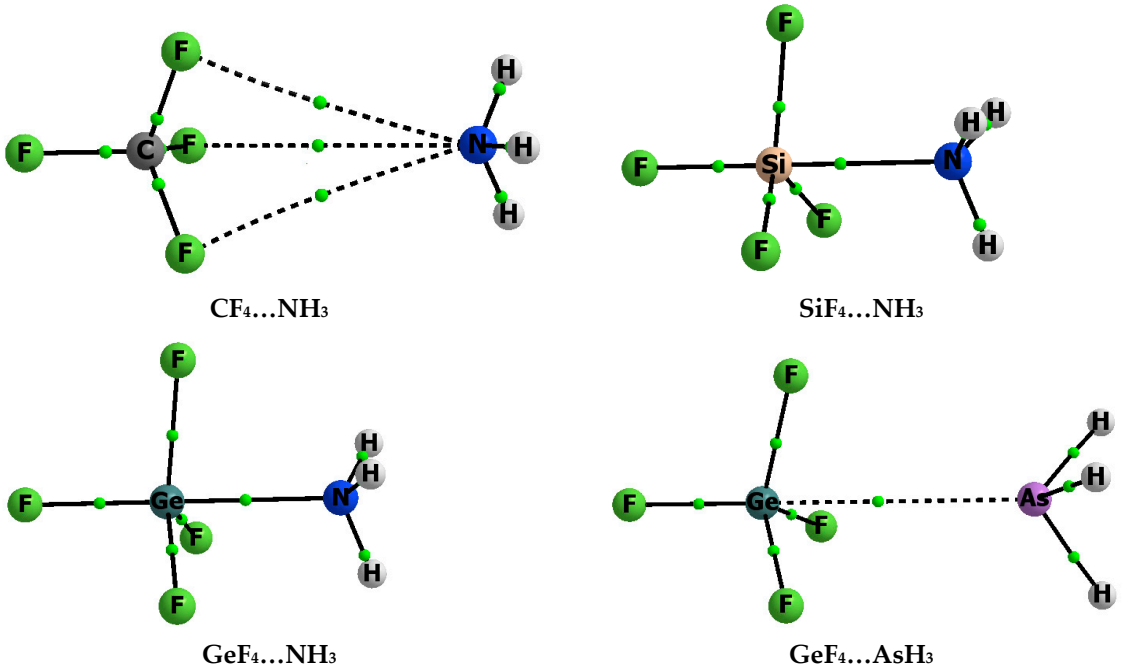

Figure 1. Molecular graphs of complexes containing one ligand (NH_3 or AsH_3); attractors are designated by big circles while bond critical points by small ones, and continuous and broken lines correspond to bond paths.

Figures 1 and 2 show bond paths (BPs) that, according to the Bader theory, correspond to stabilizing interactions [50,51]; Z-centres are characterized by four Z-F bond paths and additionally by one or two Z–N(As) BPs, for complexes with one or two ligands, respectively. The latter bond paths correspond to the interactions between the tetrel σ-hole and electron reach nitrogen or arsenic centre. The CF_4–NH_3 complex is the only exception since the N-attractor of NH_3 is not connected with the

carbon but with the fluorine attractors by three BPs (Figure 1) that seems to be surprising because the F-atoms are characterized by the negative EP. However, the local F–N electrostatic repulsions are rather weak here since the EP at F-centres of CF_4 is equal to only −0.002 au. It seems that the F–N bond paths correspond to stabilizing interactions, which are ruled by dispersive forces. These conclusions are partly confirmed by results presented in Table 1. The E_{int} for the CF_4–NH_3 complex is equal to −1.1 kcal/mol that shows a very weak interaction between the CF_4 and NH_3 species. This weak interaction is accompanied by the absence of the deformation being the result of complexation, i.e., the E_{def} is equal to zero. The similar weak interaction, where the CF_4 unit is in contact with the nitrogen centre, was found for the pyridine–CF_4 complex where the dissociation energy is lower than 1 kcal/mol [52].

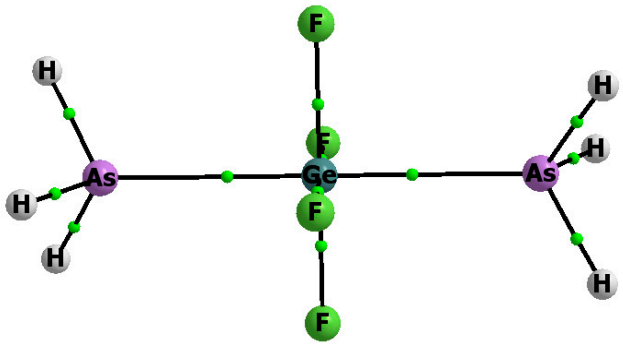

GeF_4…$(AsH_3)_2$

Figure 2. Molecular graph of the GeF_4–$(AsH_3)_2$ complex; attractors are designated by big circles while bond critical points by small ones, and continuous lines correspond to bond paths.

Much stronger interactions are observed for remaining complexes (Table 1); for those containing one ligand, the strength of interaction increases with the increase of the atomic number of Z-centre; for the ZF_4–NH_3 complexes, E_{int} is equal to −1.1, −29.6 and −33.8 kcal/mol for Z = C, Si and Ge, respectively. Table S1 (Supplementary Materials) shows all interaction and binding energies including calculations where relativistic effects were not taken into account for complexes containing Ge and As atoms. The results show that differences between energies with relativistic corrections and without them are not meaningful.

Table 1. The energetic parameters (in kcal/mol); the interaction energy, E_{int}, and the binding energy, E_{bin}, corrected for BSSE, the deformation energy, E_{def}. The tetrel–Lewis base centre distances are included, Z–B (i.e., Z–N or Z–As, Z = C, Si, Ge, in Å).

Complex	Z–B	E_{int}	E_{bin}	BSSE	E_{def}
CF_4–NH_3	3.658	−1.1	−1.1	0.3	0.0
CF_4–$(NH_3)_2$	1.658	−29.1	90.1	3.0	119.2
CF_4–$(NH_3)_2$ *	1.658	−76.8	91.9	6.5	168.7
SiF_4–NH_3	2.072	−29.6	−8.5	2.5	21.1
SiF_4–$(NH_3)_2$	1.940	−44.4	−14.7	2.4	29.7
SiF_4–$(NH_3)_2$ *	1.940	−93.9	−23.7	4.4	70.2
GeF_4–NH_3	2.080	−33.8	−16.2	4.7	17.6
GeF_4–$(NH_3)_2$	1.997	−42.4	−19.2	4.9	23.2
GeF_4–$(NH_3)_2$ *	1.997	−90.5	−34.2	10.9	56.3
GeF_4–AsH_3	3.399	−2.8	−1.8	1.9	1.0
GeF_4–$(AsH_3)_2$	2.543	−22.3	10.3	5.1	32.6
GeF_4–$(AsH_3)_2$ *	2.543	−48.1	11.5	10.1	59.6

* Interaction and binding energies are related to three components (see text for explanation).

The C < Si < Ge order of an increase of the electrostatic potential at the tetrel centre for the tetrel tetrafluorides is observed with the following EP maxima: +0.034, +0.072 and +0.086 au, respectively (Table S2), which is in agreement with the above-mentioned increase of the strength of interaction between the ZF_4 and NH_3 species. It is worth mentioning that, in complexes with one ligand (Figure 1), there are three linearly located N(As)–Z–F atoms while the ZF_3 central part is not planar like for the perfect trigonal bipyramidal geometry. The order of an increase of E_{bin} values for the ZF_4–NH_3 complexes is the same as for E_{int}.

One can see large E_{def} values for the SiF_4–NH_3 and GeF_4–NH_3 complexes, equal to 21.1 and 17.6 kcal/mol, respectively; these values correspond to large geometrical changes being a result of complexation. Figure 3 defines the α-angle which for the ZF_4 species not involved in any interaction should be equal to 70.5° corresponding to the perfect tetrahedral geometry. However, this angle increases with the increase of a strength of interaction with the Lewis base centre. It was justified that the tetrel bond may be considered as a preliminary stage of the S_N2 reaction [12]; α-angle is equal to 90° or nearly so for the transition state of this reaction. Figure 3 shows that α is greater for the SiF_4–NH_3 and GeF_4–NH_3 complexes than for the CF_4–NH_3 and GeF_4–AsH_3 ones; the latter complexes are characterized by weaker interactions and lower deformation energies than the former complexes. Table 1 also shows that the Z–N(As) distance is close to 2 Å for strong interactions in the SiF_4–NH_3 and GeF_4–NH_3 complexes while this value exceeds 3 Å for the CF_4–NH_3 and GeF_4–AsH_3 moieties.

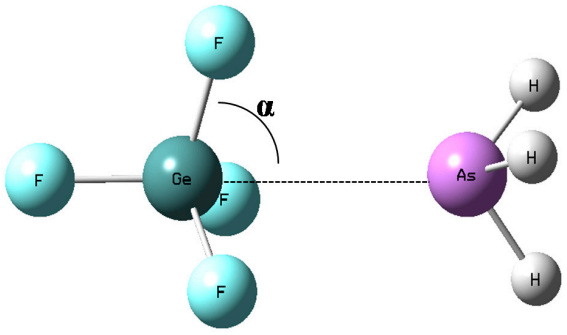

Complex	α [°]
CF_4…NH_3	70.9
SiF_4…NH_3	82.8
GeF_4…NH_3	83.2
GeF_4…AsH_3	73.5

Figure 3. The definition of the α-angle, the GeF_4–AsH_3 complex is presented as an example, the α-angles for complexes containing one ligand are given, this angle for all complexes with two ligands is equal to 90° or nearly so.

Stronger Z–N(As) interactions are observed for complexes containing two ligands than for corresponding complexes containing one ligand (Table 1, E_{int} values). The energy of interaction, similar to the binding energy, for the complex containing two ligands refers to two components (treated as monomers): ligand (NH_3 or AsH_3) and the complex containing one ligand (ZF_4–NH_3 or GeF_4–AsH_3). The E_{int} calculated in such a way for ZF_4–$(NH_3)_2$ is equal to −29.1, −44.4 and −42.4 kcal/mol for Z = C, Si and Ge, respectively; this energy for the GeF_4–$(AsH_3)_2$ complex is equal to −22.3 kcal/mol. The stronger interactions for complexes with two ligands correspond to shorter Z–N(As) distances than the corresponding distances for complexes containing one ligand (Table 1).

Table 1 shows the positive binding energies for the CF_4–$(NH_3)_2$ and GeF_4–$(AsH_3)_2$ complexes. These complexes are in energetic minima, like all systems analysed here, however the positive E_{bin} values indicate that the additional second ligand leads to the system energetically less favourable than the reaction subtracts. Table 1 also presents, for complexes containing two ligands, the interaction

and binding energies related to three subtracts; this means that E_{int} is calculated as the difference between the energy of the complex and the sum of energies of three components (two ligands and ZF_4). The binding energy is also positive for the CF_4–$(NH_3)_2$ and GeF_4–$(AsH_3)_2$ complexes.

The α angle for all complexes with two ligands is equal to 90°, or nearly so, and the ZF_4 fragments of these complexes are planar; thus there is the central ZF_4 fragment here with two ligands situated in the N(As)–Z–N(As) line that corresponds to the octahedral structure (Figure 2). Structures with the hexacoordinated tetrel centre that are not characterized by the regular octahedron are also observed. For example, such a situation was observed for the ZF_4–$(CH_3CN)_2$ complexes (Z = Si, Ge) where the ZF_4 fragments are far from planarity and their tetrahedral structures are not distorted significantly [20]. The SiF_4–$(NH_3)_2$ complex is another example [9] where four fluorines and two nitrogens constitute a distorted octahedron around the silicon and the N–Si–N angle is equal to 89°; this angle is equal to 180° for the regular octahedral conformation analysed here.

3.2. Electron Charge Shifts Resulting from Complexation—QTAIM Approach

Table 2 presents characteristics of the Z–N(As) bond critical point (BCP). The parameters of BCP characterize an interaction considered; numerous analyses of BCPs were performed for the hydrogen bonded systems [6,53]. For example, the electron density at BCP—ρ_{BCP} often correlates with the strength of the corresponding interaction that is usually expressed by the interaction or binding energy [53]. The latter correlations are usually observed for homogenous samples of complexes and for interactions between pairs of the same type atoms. For the Z–N(As) contacts analysed here the Z-centre concerns different Group 14 elements; however, one can see (Table 2) that the Z–N(As) ρ_{BCP} is greater for complexes containing two ligands than for corresponding complexes with one ligand. This is in line with the strength of interactions that are stronger for complexes with two ligands. Two Z–N(As) BCPs for each complex with two ligands are equivalent due to the symmetry of these species. There are the lowest ρ_{BCP} values of 0.003 and 0.012 au for the CF_4–NH_3 and GeF_4–AsH_3 complexes where the weakest interactions are observed (Table 1).

Table 2. The QTAIM characteristics (in au) of the Z–N(As) BCP (Z = C, Si, Ge); electron density at BCP, ρ_{BCP}, its Laplacian, $\nabla^2\rho_{BCP}$, the total electron energy density at BCP, H_{BCP}, the potential electron energy density at BCP, V_{BCP}, the kinetic electron energy density at BCP, G_{BCP}.

Complex	ρ_{BCP}	V_{BCP}	G_{BCP}	H_{BCP}	$\nabla^2\rho_{BCP}$
CF_4–NH_3 *	0.003	−0.002	0.002	0.001	0.012
CF_4–$(NH_3)_2$	0.183	−0.211	0.069	−0.142	−0.292
SiF_4–NH_3	0.062	−0.098	0.074	−0.024	0.200
SiF_4–$(NH_3)_2$	0.081	−0.147	0.113	−0.033	0.319
GeF_4–NH_3	0.083	−0.117	0.081	−0.036	0.184
GeF_4–$(NH_3)_2$	0.098	−0.153	0.106	−0.047	0.235
GeF_4–AsH_3	0.012	−0.006	0.006	0.000	0.026
GeF_4–$(AsH_3)_2$	0.062	−0.052	0.028	−0.025	0.012

* Concerns one of three F–N contacts.

The negative Laplacian of the electron density at BCP, $\nabla^2\rho_{BCP}$, indicates the electron density concentration in the inter-atomic region that corresponds to a covalent bond [44,45]. On the other hand, the positive Laplacian value shows the depletion of the electron density that corresponds to the closed–shell interaction. Table 2 shows the negative Laplacian only for C–N contacts in the CF_4–$(NH_3)_2$ complex. For the latter complex, the negative values of $\nabla^2\rho_{BCP}$ for C-F bonds are also observed (Table S3 presents BCP characteristics of the Z-F bond). Thus, according to the QTAIM approach, there is a hexavalent carbon centre in the CF_4–$(NH_3)_2$ complex. The negative $\nabla^2\rho_{BCP}$ is also observed for C-F bonds in the CF_4–NH_3 complex (Table S3); however, the C–N bond path is not observed there (Figure 1).

For numerous molecular systems $\nabla^2\rho_{BCP} > 0$ and $H_{BCP} < 0$; it was stated that these relations are a sufficient condition to classify any interaction as a covalent bond or at least as an interaction partly covalent in nature [54–56]. Table 2 shows the negative H_{BCP} values for the Z–N(As) contacts for almost all complexes analysed here, except for the CF_4–NH_3 complex, where the C–N bond path is not observed, and the GeF_4–AsH_3 complex; both complexes are weakly bonded since the H_{BCP} values for BCPs of the F–N and Ge–As bond paths, respectively, are positive and close to zero. Table S3 shows the negative $\nabla^2\rho_{BCP}$ values for the C-F bonds for complexes of the CF_4 species; for all remaining complexes, the Z-F $\nabla^2\rho_{BCP}$ and H_{BCP} values are positive and negative, respectively, which means that, according to the QTAIM approach, only for the CF_4–$(NH_3)_2$ complex the hypervalency (hexavalent carbon) is observed without any doubt; for the CF_4–NH_3 and GeF_4–AsH_3 complexes the carbon and germanium centres are tetravalent ones while for the remaining species the negative H_{BCP} values show that this phenomenon may be taken into account. To illustrate the above situation, Figure 4 shows the molecular graphs with the reactive surfaces ($\nabla^2\rho(r) = 0$) for the CF_4–$(NH_3)_2$ and SiF_4–$(NH_3)_2$ complexes.

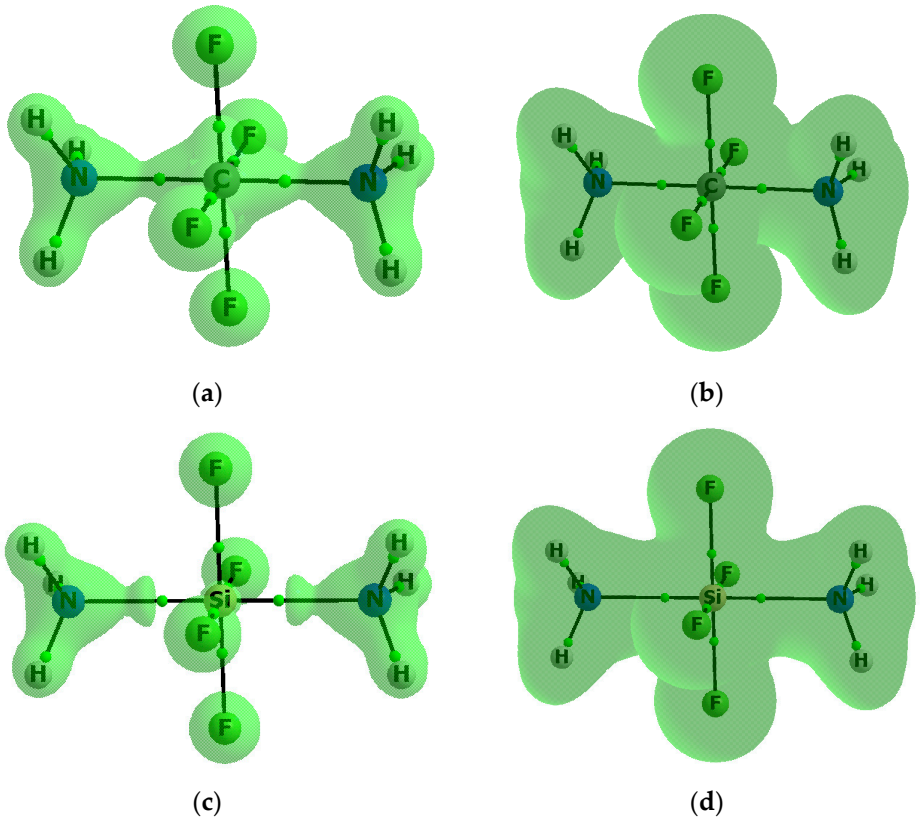

Figure 4. The molecular graph of the: CF_4–$(NH_3)_2$ complex (**a**,**b**); and the SiF_4–$(NH_3)_2$ complex (**c**,**d**). Solid lines correspond to bond paths, big circles to attractors and small green circles to BCPs; the reactive surfaces based on the Laplacian of electron density ($\nabla^2\rho(r) = 0$ isosurfaces (**a**,**c**)) and based on the total electron energy density (H(r) = 0 isosurfeces (**b**,**d**)).

The areas closed by these surfaces are regions of the electron density concentration. One can see that for the CF_4–$(NH_3)_2$ complex the N–C–N line (i.e., both N–C contacts) is located in the region of the negative Laplacian, also the BCPs of all C-F bonds are located in such regions, thus the hexavalent C-centre is observed for this complex. For the SiF_4–$(NH_3)_2$ complex, all BCPs, corresponding to the Si–N contacts and to the Si-F bonds, are located in regions of the positive Laplacian; however, as described earlier here, all corresponding H_{BCP} values are negative. On the other hand, for both complexes presented in Figure 4, all fluorine centres with their spheres of the negative Laplacian are

separated from the remaining parts of complexes, which may suggest the strong polarization of Z-F bonds, as is discussed below. Figure 4 also presents the reactive surfaces based on the total electron energy densities (H(r) = 0) where for both CF_4–$(NH_3)_2$ and SiF_4–$(NH_3)_2$ complexes all Z-F and Z–N links are located in regions of the negative H-values. This means that the sharp criterion of covalency based on the negative Laplacian leads to the conclusion that the carbon in the CF_4–$(NH_3)_2$ is hexavalent but the silicon in the SiF_4–$(NH_3)_2$ complex is not. However, if the criterion of covalency based on the negative H-value is applied to the carbon and silicon centres, the above-mentioned complexes are hexavalent ones. It is worth mentioning that the covalency of Si–N interactions for the SiF_4–$(NH_3)_2$ complex were suggested early on [18]. However, this analysis was based only on the energetic and geometric parameters resulting from ab initio MO calculations with the use of not saturated STO-3G and STO-6G basis sets [18].

3.3. Electron Charge Shifts Resulting from Complexation—NBO Approach

Table 3 presents NBO parameters for the ZF_4 monomers and for their complexes with one and two ligands; the NBO charges and the polarizations of Z-F bonds and of Z–N(As) contacts (denoted as PLs) are presented; the Z-F bond lengths are also included. Q_{ZF4} is the NBO charge of the ZF_4 moiety; for isolated monomers, it is equal to zero but in complexes the ZF_4 species withdraws the electron density from ligands due to its Lewis acid properties. More negatively charged ZF_4 fragment is observed for complexes containing two ligands than for the corresponding complexes with one ligand. For the CF_4–NH_3 and GeF_4–AsH_3 complexes characterized by the weakest interactions, the lowest electron density transfer is observed; even for the former complex, such transfer is not observed which may support previous conclusions that this complex is stable due to weak dispersive forces. Q_F is the fluorine charge in the ZF_4 fragment. For the ZF_4 monomers and for the complexes with two ligands, all F-atoms in the species considered possess the same atomic charge due to the symmetry constraints. The situation is different for complexes with one ligand where the F-atom located in F-Z–N(As) line possesses slightly different charge than the remaining F-atoms (Table 3).

For the T_d symmetry isolated CF_4 species, all F-centres possess the charge of -0.316 au, while, in the CF_4–NH_3 complex where the electron charge density transfer from the NH_3 ligand is not observed, the charge for F-atom situated in the F-C–N line is equal to -0.358 au while the charges of remaining F-atoms are equal to -0.349 au. Additionally, the carbon centre in this complex possesses the charge amounting +1.404 au while for the isolated CF_4 species it is equal to +1.264 au, which means that, in the CF_4–NH_3 complex, despite the lack of intermolecular electron charge density shift from NH_3 to CF_4 ($Q_{CF4} = 0$), the electron density redistribution within CF_4 is observed, showing the significance of polarization effects. One can see that the increase of the positive charge of the Z centre in the complex in comparison with the isolated ZF_4 species is observed for all complexes containing one ligand (Table 3). For complexes with two ligands, the decrease of the positive charge of Z-centre is observed—this charge is lower than for complexes with one ligand and even lower than for the corresponding isolated ZF_4 molecules.

Table 3. The NBO characteristics; charges (in au) and polarizations (percentage of the electron density at Z-centre, Z = C, Si, Ge); and the Z-F bond lengths (Å) are also included. Q_{ZF4}, the charge of the ZF_4 moiety; Q_F, the charge of the F-atom; Q_Z, the charge of Z-centre; PL_{ZF}, polarization of the Z-F bond; and PL_{ZB}, polarization of the Z-B (B = N, As) contact.

Moiety	Q_{ZF4}	Q_F *	Q_Z	PL_{ZF} *	Z-F *	PL_{ZB}
CF_4	0	−0.316	1.264	28.7	1.321	not applied
CF_4–NH_3	0	−0.349 (−0.358)	1.404	28.7 (28.5)	1.319 (1.327)	no occurrence
CF_4–$(NH_3)_2$	−1.111	−0.522	0.977	17.7	1.559	22.8
SiF_4	0	−0.634	2.537	12.4	1.574	not applied
SiF_4–NH_3	−0.163	-0.692 (−0.696)	2.608	11.1(10.4)	1.610 (1.612)	6.8
SiF_4–$(NH_3)_2$	−0.467	−0.717	2.399	9.7	1.675	9.7
GeF_4	0	−0.628	2.511	13.5	1.687	not applied
GeF_4–NH_3	−0.183	−0.706 (−0.704)	2.640	10.9 (10.2)	1.724 (1.719)	7.0
GeF_4–$(NH_3)_2$	−0.465	−0.735	2.476	8.5	1.776	8.8
GeF_4–AsH_3	−0.017	−0.684 (−0.691)	2.727	12.7 (12.4)	1.691 (1.694)	no occurrence
GeF_4–$(AsH_3)_2$	−0.738	−0.733	2.195	8.5	1.769	14.9

* The Z-F bond length, its polarization (PL_{ZF}), and the F-charge (Q_F) of the bond situated approximately at the F-Z–N(As) line are given in parentheses.

The increase of the positive charge of Z-centre and the increase of the negative charge of F-atom situated in the F-Z–N line shows the mechanism corresponding to that one occurring for the A-H–B hydrogen bond formation [47,57]. In the case of the A-H–B hydrogen bond, the complexation usually leads to the increase of the positive charge of H-atom and to the increase of the negative charge of A-centre [47]; this is connected with two mechanisms steering the H-bond formation; the hyperconjugative A-H bond weakening and the rehybridization-promoted A-H bond strengthening [57].

Table 3 presents bond polarizations calculated as the percentage of the electron density at the Z-centre—it concerns Z–N/As contacts as well as Z-F bonds. It is interesting that most Z–N(As) contacts are classified as covalent bonds within NBO approach since the Z-N(As) bond orbitals are observed here; only for two complexes characterized by the weakest interactions, CF_4–NH_3 and GeF_4–AsH_3, such orbitals are not observed. The polarizations of these Z-N(As) bonds within NBO approach show a large electron density shift to N(As)-atoms, the lowest shift but still significant is observed for the CF_4–$(NH_3)_2$ complex where polarization amounts 22.8%. The significant electron density shifts from Z-centres to F-atoms are also detected for Z-F bonds with the lowest shifts for the CF_4–NH_3 complex; the C-F bond polarizations are close here to 29%.

One can see that the F-Z–N/As tetrel bonds analysed here are classified as strong ones characterized by the significant contribution of covalency. The latter is confirmed by the NBO and QTAIM approaches, most of interactions may be even classified as strongly polarized covalent bonds. For weaker A-Z–B tetrel bonds analysed previously the most important $n(B) \rightarrow \sigma^*_{AZ}$ orbital–orbital interaction is observed [12], where B is the electron donating Lewis base centre while Z is the tetrel atom connected with any A-centre. This is the overlap between the lone pair B-orbital, n(B), and the antibonding A-Z orbital, σ^*_{AZ}. The analogue situation occurs for the A-H–B hydrogen bond where the $n(B) \rightarrow \sigma^*_{AH}$ orbital–orbital interaction is a signature of the H-bond formation [47,57].

For two complexes analysed here, where Z-N(As) bond orbitals were not detected, the following situation is observed. For the CF_4–NH_3 complex, the orbital–orbital interactions between CF_4 and NH_3 are not detected at all. This corresponds to the weak intermolecular interaction and to the lack of the intermolecular electron charge density shift (Table 3). For the GeF_4–AsH_3 complex, the strongest orbital–orbital interaction of 2.4 kcal/mol occurs for the $n(As) \rightarrow n^*(Ge)$ overlap. One can see that the orbital–orbital interactions for the CF_4–NH_3 and GeF_4–AsH_3 complexes do not follow the typical tetrel bonds [12].

3.4. ZF_4 Moiety in Crystal Structures

Cambridge Structural Database (CSD) [58] searches were performed. The following search criteria were used: no disordered structures, no structures with unresolved errors, no powder structures, no polymeric structures, and R $\leq$ 7.5%.

To analyse systems structurally close to the complexes described here, searches for CF_4, SiF_4 and GeF_4 species connected with two Lewis base ligands were performed. Hence, for the above tetrel centres, additional contacts with the Groups 15 and 16 elements were searched. In other words, the following fragments were considered: $CF_4L^1L^2$, $SiF_4L^1L^2$ and $GeF_4L^1L^2$ where L^1 and L^2 are any ligands attached to C, Si or Ge by atoms of the Groups 15 and/or 16 element. Carbon $CF_4L^1L^2$ structures were not found; nine silicon centre crystal structures were found; and 13 germanium centre crystal structures were found. Figure 5 presents few examples of such structures with the corresponding Refcodes.

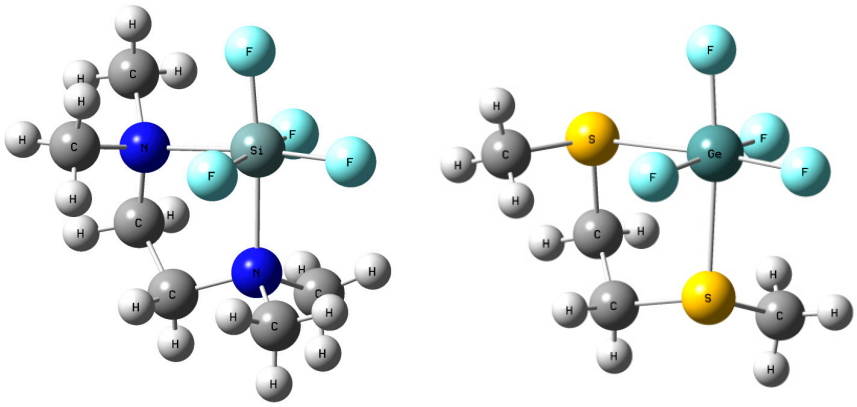

DOWNIM **TIVVUQ**

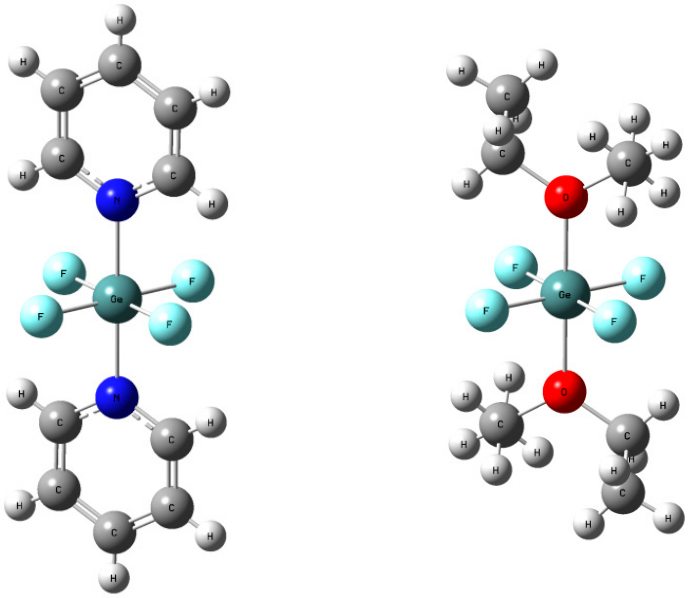

HUMCOH01 **MEQZEN**

Figure 5. Examples of crystal structures containing hexacoordinated Si or Ge centre, the $SiF_4L^1L^2$ and $GeF_4L^1L^2$ arrangements are considered (L^1 and L^2—ligands connected with Si or Ge by the Groups 15 and 16 element); the Cambridge Structural Database Refcodes are shown.

For the silicon structures in three cases, the non-fluorine ligands are situated in axial positions, like for the SiF_4-$(NH_3)_2$ conformation analysed in this study. For the remaining six silicon structures the lig-Si-lig angle (lig designates the Lewis base ligand centre) is close to 90° (Figure 5, DOWNIM Refcode is an example) like for the SiF_4-$(NH_3)_2$ conformer reported by Politzer and co-workers [9]. However, all nine silicon structures are perfect octahedrons or nearly so. For the germanium structures, in six cases the non-fluorine ligands are situated in axial positions (Figure 5, HUMCOH01 and MEQZEN) while for the remaining seven structures the lig-Ge-lig angle is close to 90° (Figure 5, TIVVUG). Similar to the silicon structures for the Ge-complexes with axial position of non-fluorine ligands, almost perfect octahedron is observed, while, for the remaining germanium complexes, it is deformed octahedron but only slightly.

4. Conclusions

The most important conclusion arises that the hypervalent tetrel centres are detected for almost all complexes analysed here, the CF_4–NH_3 and GeF_4–AsH_3 complexes are the only exceptions (here the tetrel centre is tetravalent). This conclusion is based on the total electron energy densities at BCPs, H_{BCP}s (QTAIM approach), and on the existence of the ligand–tetrel centre bond orbitals (NBO method). One can observe pentavalent or hexavalent tetrel centres if complexes with one and two ligands are analysed, respectively. However, the tetrel–ligand and Z-F bonds for these complexes are strongly polarized, which means that a large outflow of the electron density from the tetrel atom to the bonded centres, F-atoms and ligands, occurs. Table 3 shows the following trend of the increase of the negative charge of F-atoms: ZF_4, ZF_4–ligand, and ZF_4–two ligands. The latter is accompanied by the change of the polarization of Z-F bonds, which means that the percentage of the electron density for the Z-F bonds at the Z-centre decreases in the same order following the increase of the negative charge of F-atom. These conclusions are in agreement with earlier statements [59,60] that, for molecules usually classified as hypervalent, the electronegativity of ligands should be taken into account [60].

The results presented in this study reveal that complexes with two ligands which possess tetrel centre that may be classified as hexavalent are more stable than complexes containing one ligand where a pentavalent tetrel centre occurs. This stability is related to the electron charge density shifts, particularly to the polarization of bonds of the Z-centre. The hexacoordinated tetrel centres (silicon and germanium) are observed in crystal structures showing that the octahedral structure is an energetically stable motif, which is important in crystal structure engineering.

Supplementary Materials: The following are available online at www.mdpi.com/2073-4352/7/2/43/s1. Figure S1: The maps of the electrostatic potential (EP) calculated at the 0.001 au molecular electron density surfaces for ZF_4; red and blue colors correspond to negative and positive EP, respectively; MP2/aug-cc-pVTZ level of calculations; Table S1: The energetic parameters (in kcal/mol); the interaction energy, E_{int}, and the binding energy, E_{bin}, corrected for BSSE, the deformation energy, E_{def}. The tetrel—Lewis base centre distances are included, Z–B (i.e., Z–N or Z–As; Z = C, Si, Ge, in Å); Table S2: Electrostatic potential local maxima and minima for ZF_4, ZF_4–NH_3 and GeF_4–AsH_3 species (in au); for the species containing Ge and As centers these values are the same if relativistic effects are taken into account; in a case of ZF_4–NH_3 complexes the local maximum is indicated since the global EP maximum corresponds to H-centers, in a case of the GeF_4–AsH_3 complex that is the global EP maximum; the EP results for the surfaces of the electron density of 0.001 au are presented; Table S3: The QTAIM characteristics (in au) of the Z-F bond critical point; electron density at BCP, ρ_{BCP}, its laplacian, $\nabla^2\rho_{BCP}$, the total electron energy density at BCP, H_{BCP}, the potential electron energy density at BCP, V_{BCP}, the kinetic electron energy density at BCP, G_{BCP}

Acknowledgments: Financial support comes from Eusko Jaurlaritza (GIC IT-588-13) and the Spanish Office for Scientific Research (CTQ2012-38496-C05-04). Technical and human support provided by Informatikako Zerbitzu Orokora—Servicio General de Informática de la Universidad del País Vasco (SGI/IZO-SGIker UPV/EHU), Ministerio de Ciencia e Innovación (MICINN), Gobierno Vasco Eusko Jaurlanitza (GV/EJ), and European Social Fund (ESF) is gratefully acknowledged.

Conflicts of Interest: The author declares no conflict of interest.

References

1. Scheiner, S. (Ed.) *Molecular Interactions. From van der Waals to Strongly Bound Complexes*; John Wiley & Sons: Chichester, UK, 1997.
2. Schneider, H.-J. Binding Mechanisms in Supramolecular Chemistry. *Angew. Chem. Int. Ed.* **2009**, *48*, 3924–3977.
3. Hobza, P.; Müller-Dethlefs, K. *Non-Covalent Interactions, Theory and Experiment. Royal Society of Chemistry*; Thomas Graham House, Science Park, Milton Road: Cambridge, UK, 2010.
4. Jeffrey, G.A.; Saenger, W. *Hydrogen Bonding in Biological Structures*; Springer: Berlin, Germany, 1991.
5. Jeffrey, G.A. *An Introduction to Hydrogen Bonding*; Oxford University Press: New York, NY, USA, 1997.
6. Grabowski, S.J.; Leszczynski, J. (Eds.) *Hydrogen Bonding—New Insights; Volume 3 of the Series: Challenges and Advances in Computational Chemistry and Physics*; Springer: Berlin, Germany, 2006.
7. Grabowski, S.J. (Ed.) *Analysis of Hydrogen Bonds in Crystals (Printed Edition of the Special Issue Published in Crystals)*; MDPI: Basel, Switzerland; Beijing/Wuhan, China; Barcelona, Spain, 2016.
8. Murray, J.S.; Lane, P.; Politzer, P. Expansion of the σ-hole concept. *J. Mol. Model.* **2009**, *15*, 723–729. [CrossRef] [PubMed]
9. Politzer, P.; Murray, J.S.; Lane, P.; Concha, M.C. Electrostatically driven complexes of SiF_4 with amines. *Int. J. Quantum Chem.* **2009**, *109*, 3773–3780. [CrossRef]
10. Bundhun, A.; Ramasami, P.; Murray, J.S.; Politzer, P. Trends in σ-hole strengths and interactions of F3MX molecules (M = C, Si, Ge and X = F, Cl, Br, I). *J. Mol. Model.* **2012**, *19*, 2739–2746. [CrossRef] [PubMed]
11. Bauzá, A.; Mooibroek, T.J.; Frontera, A. Tetrel-Bonding Interaction Rediscovered Supramolecular Force? *Angew. Chem. Int. Ed.* **2013**, *52*, 12317–12321. [CrossRef] [PubMed]
12. Grabowski, S.J. Tetrel bond—σ-hole bond as a preliminary stage of the S_N2 reaction. *Phys. Chem. Chem. Phys.* **2014**, *16*, 1824–1834. [CrossRef] [PubMed]
13. Politzer, P.; Murray, J.S.; Clark, T. Halogen bonding: An electrostatically-driven highly directional noncovalent interaction. *Phys. Chem. Chem. Phys.* **2010**, *12*, 7748–7758. [CrossRef] [PubMed]
14. Politzer, P.; Murray, J.S.; Clark, T. Halogen bonding and other σ-hole interactions: A perspective. *Phys. Chem. Chem. Phys.* **2013**, *15*, 11178–11189. [CrossRef] [PubMed]
15. Politzer, P.; Murray, J.S. Halogen Bonding: An Interim Discussion. *ChemPhysChem* **2013**, *14*, 2145–2151. [CrossRef] [PubMed]
16. Politzer, P.; Murray, J.S.; Janjić, G.V.; Zarić, S.D. σ-Hole Interactions of Covalently-Bonded Nitrogen, Phosphorus and Arsenic: A Survey of Crystal Structures. *Crystals* **2014**, *4*, 12–31. [CrossRef]
17. Bauzá, A.; Frontera, A. Aerogen Bonding Interaction: A New Supramolecular Force? *Angew. Chem. Int. Ed.* **2015**, *54*, 7340–7343. [CrossRef] [PubMed]
18. Chehayber, J.M.; Nagy, S.T.; Lin, C.S. Ab initio studies of complexes between SF_4 and ammonia. *Can. J. Chem.* **1984**, *62*, 27–31. [CrossRef]
19. Alkorta, I.; Rozas, I.; Elguero, J. Molecular Complexes between Silicon Derivatives and Electron-Rich Groups. *J. Phys. Chem. A* **2001**, *105*, 743–749. [CrossRef]
20. Helminiak, H.M.; Knauf, R.R.; Danforth, S.J.; Phillips, J.A. Structural and Energetic Properties of Acetonitrile–Group IV (A & B) Halide Complexes. *J. Phys. Chem. A* **2014**, *118*, 4266–4277. [PubMed]
21. Sedlak, R.; Stasyuk, O.A.; Fonseca Guerra, C.; Rézač, J.; Růžička, A.; Hobza, P. New Insight into the Nature of Bonding in the Dimers of Lappert's Stannylene and Its Ge Analogs: A Quantum Mechanical Study. *J. Chem. Theory Comput.* **2016**, *12*, 1696–1704. [CrossRef] [PubMed]
22. Grabowski, S.J. Tetrel bonds, penta- and hexa-coordinated tin and lead centres. *Appl. Organometal. Chem.* **2017**, e3727. [CrossRef]
23. Yamashita, M.; Yamamoto, Y.; Akiba, K.-Y.; Hashizume, D.; Iwasaki, F.; Takagi, N.; Nagase, S. Syntheses and Structures of Hypervalent Pentacoordinate Carbon and Boron Compounds Bearing an Anthracene Skeleton—Elucidation of Hypervalent Interaction Based on X-ray Analysis and DFT Calculation. *J. Am. Chem. Soc.* **2005**, *127*, 4354–4371. [CrossRef] [PubMed]
24. Akiba, K.-Y.; Moriyama, Y.; Mizozoe, M.; Inohara, H.; Nishii, T.; Yamamoto, Y.; Minoura, M.; Hashizume, D.; Iwasaki, F.; Takagi, N.; et al. Synthesis and Characterization of Stable Hypervalent Carbon Compounds (10-C-5) Bearing a 2,6-Bis(*p*-substituted phenyloxymethyl)benzene Ligand. *J. Am. Chem. Soc.* **2005**, *127*, 5893–5901. [CrossRef] [PubMed]

25. Akiba, K. *Hypervalent Carbon Compounds: Can Hexavalent Carbon Exist? In Organo Main Group Chemistry*; Akiba, K., Ed.; John Wiley & Sons, Inc.: Hoboken, NJ, USA, 2011; Chapter 12; pp. 251–268.
26. Sohail, M.; Panisch, R.; Bowden, A.; Bassindale, A.R.; Taylor, P.G.; Korlyukov, A.A.; Arkhipov, D.E.; Male, L.; Callear, S.; Coles, S.J.; et al. Pentacoordinate silicon complexes with dynamic motion resembling a pendulum on the S_N2 reaction pathway. *Dalton Trans.* **2013**, *42*, 10971–10981. [CrossRef] [PubMed]
27. Pelzer, S.; Neumann, B.; Stammler, H.-G.; Ignat'ev, N.; Hoge, B. Synthesis of bis(pentafluoroethyl)germanes. *Chem. Eur. J.* **2016**, *22*, 4758–4763. [CrossRef] [PubMed]
28. Pelzer, S.; Neumann, B.; Stammler, H.-G.; Ignat'ev, N.; Hoge, B. Hypervalent Pentafluoroethylgermanium Compounds, $[(C_2F_5)_nGeX_{5-n}]^-$ and $[(C_2F_5)_3GeF_3]^{2-}$ (X = F, Cl; n = 2–5). *Chem. Eur. J.* **2016**, *22*, 16460–16466. [CrossRef] [PubMed]
29. Bouška, M.; Dostal, L.; Růžička, A.; Jambor, R. Stabilization of Three-Coordinated Germanium(II) and Tin(II) Cations by a Neutral Chelating Ligand. *Organometallics* **2013**, *32*, 1995–1999. [CrossRef]
30. Miller, D.B.; Sisler, H.H. Observations on the Addition Compound of Silicon Tetrafluoride and Ammonia. *J. Am. Chem. Soc.* **1955**, *77*, 4998–5000. [CrossRef]
31. Ault, B.S. Matrix-isolation studies of Lewis acid/base interactions: Infrared spectra of the 1:1 adduct $SiF_4.NH_3$. *Inorg. Chem.* **1981**, *20*, 2817–2822. [CrossRef]
32. Urban, R.-D.; Rouillé, G.; Takami, M. Free jet IR spectroscopy of SiF_4-N_2 and SiF_4-CO complexes in the 10 μm region. *J. Mol. Struct.* **1997**, *413–414*, 511–519. [CrossRef]
33. Walther, A.M.; Ault, B.S. Infrared matrix isolation study of intermediate molecular complexes: Complexes of tetrafluorogermane with oxygen-containing bases. *Inorg. Chem.* **1984**, *23*, 3892–3897. [CrossRef]
34. Davis, M.F.; Levason, W.; Reid, G.; Webster, M.; Zhang, W. The first examples of germanium tetrafluoride and tin tetrafluoride complexes with soft thioether coordination—Synthesis, properties and crystal structures. *Dalton Trans.* **2008**, 533–538. [CrossRef] [PubMed]
35. Davis, M.F.; Levason, W.; Reid, G.; Webster, M. Complexes of germanium(IV) fluoride with phosphane ligands: Structural and spectroscopic authentication of germanium(IV) phosphane complexes. *Dalton Trans.* **2008**, *17*, 2261–2269. [CrossRef]
36. Frisch, M.J.; Trucks, G.W.; Schlegel, H.B.; Scuseria, G.E.; Robb, M.A.; Cheeseman, J.R.; Scalmani, G.; Barone, V.; Mennucci, B.; Petersson, G.A.; et al. *Gaussian 09, Revision A.1*, Gaussian, Inc.: Wallingford, CT, USA, 2009.
37. Møller, C.; Plesset, M.S. Note on an Approximation Treatment for Many-Electron Systems. *Phys. Rev.* **1934**, *46*, 618–622. [CrossRef]
38. Woon, D.E.; Dunning, T.H., Jr. Gaussian Basis Sets for Use in Correlated Molecular Calculations. III. The second row atoms, Al-Ar. *J. Chem. Phys.* **1993**, *98*, 1358–1371.
39. Metz, B.; Stoll, H.; Dolg, M. Small-core multiconfiguration-Dirac–Hartree–Fock-adjusted pseudopotentials for post-*d* main group elements: Application to PbH and PbO. *J. Chem. Phys.* **2000**, *113*, 2563–2569. [CrossRef]
40. Peterson, K.A. Systematically convergent basis sets with relativistic pseudopotentials. I. Correlation consistent basis sets for the post-d group 13–15 elements. *J. Chem. Phys.* **2003**, *119*, 11099–11112. [CrossRef]
41. Piela, L. *Ideas of Quantum Chemistry*; Elsevier Science Publishers: Amsterdam, The Netherlands, 2007; pp. 684–691.
42. Grabowski, S.J.; Sokalski, W.A. Different types of hydrogen bonds: Correlation analysis of interaction energy components. *J. Phys. Org. Chem.* **2005**, *18*, 779–784. [CrossRef]
43. Boys, S.F.; Bernardi, F. The calculation of small molecular interactions by the differences of separate total energies. Some procedures with reduced errors. *Mol. Phys.* **1970**, *19*, 553–561.
44. Bader, R.F.W. *Atoms in Molecules, A Quantum Theory*; Oxford University Press: Oxford, UK, 1990.
45. Wiley-VCH. *Quantum Theory of Atoms in Molecules: Recent Progress in Theory and Application*; Matta, C., Boyd, R.J., Eds.; Wiley-VCH: Weinheim, Germany, 2007.
46. Keith, T.A. *AIMAll (Version 11.08.23)*, TK Gristmill Software: Overland Park, KS, USA, 2011.
47. Weinhold, F.; Landis, C. *Valency and Bonding, A Natural Bond Orbital Donor—Acceptor Perspective*; Cambridge University Press: Cambridge, UK, 2005.
48. Glendening, E.D.; Badenhoop, J.K.; Reed, A.E.; Carpenter, J.E.; Bohmann, J.A.; Morales, C.M.; Weinhold, F. *NBO 5.0*, Theoretical Chemistry Institute, University of Wisconsin: Madison, WI, USA, 2001.
49. Schmidt, M.W.; Baldridge, K.K.; Boatz, J.A.; Elbert, S.T.; Gordon, M.S.; Jensen, J.H.; Koseki, S.; Matsunaga, N.; Nguyen, K.A.; Su, S.J.; et al. General Atomic and Molecular Electronic Structure System. *J. Comput. Chem.* **1993**, *14*, 1347–1363. [CrossRef]

50. Bader, R.F.W. A Bond Path: A Universal Indicator of Bonded Interactions. *J. Phys. Chem. A* **1998**, *102*, 7314–7323. [CrossRef]
51. Bader, R.F.W. Bond Paths Are Not Chemical Bonds. *J. Phys. Chem. A* **2009**, *113*, 10391–10396. [CrossRef] [PubMed]
52. Maris, A.; Favero, L.B.; Velino, B.; Caminati, W. Pyridine-CF_4: A Molecule with a Rotating Cap. *J. Phys. Chem. A* **2013**, *117*, 11289–11292. [CrossRef] [PubMed]
53. Grabowski, S.J. What is the Covalency of Hydrogen Bonding? *Chem. Rev.* **2011**, *11*, 2597–2625. [CrossRef] [PubMed]
54. Jenkins, S.; Morrison, I. The chemical character of the intermolecular bonds of seven phases of ice as revealed by AB initio calculation of electron densities. *Chem. Phys. Lett.* **2000**, *317*, 97–102. [CrossRef]
55. Arnold, W.D.; Oldfield, E. The Chemical Nature of Hydrogen Bonding in Proteins via NMR: *J*-Couplings, Chemical Shifts, and AIM Theory. *J. Am. Chem. Soc.* **2000**, *122*, 12835–12841. [CrossRef]
56. Rozas, I.; Alkorta, I.; Elguero, J. Behavior of ylides containing N, O, and C atoms as hydrogen bond acceptors. *J. Am. Chem. Soc.* **2000**, *122*, 1154–11161. [CrossRef]
57. Alabugin, I.V.; Manoharan, M.; Peabody, S.; Weinhold, F. Electronic Basis of Improper Hydrogen Bonding: A Subtle Balance of Hyperconjugation and Rehybridization. *J. Am. Chem. Soc.* **2003**, *125*, 5973–5987. [CrossRef] [PubMed]
58. Wong, R.; Allen, F.H.; Willett, P. The scientific impact of the Cambridge Structural Database: A citation-based study. *J. Appl. Cryst.* **2010**, *43*, 811–824. [CrossRef]
59. Gillespie, R.J. Fifty years of the VSEPR model. *Coord. Chem. Rev.* **2008**, *252*, 1315–1327. [CrossRef]
60. Gillespie, R.J.; Popelier, P.L.A. *Chemical Bonding and Molecular Geometry*; Oxford University Press: Oxford, UK, 2001.